For publication in the *Terrestrial, Atmospheric, and Oceanic Sciences*, 1999

On two methods using magnetometer-array data for studying magnetic pulsations

P. J. Chi and C. T. Russell
Institute of Geophysics and Planetary Physics, University of California, Los Angeles

KEYWORDS: ULF waves, field line resonances, cross-phase spectrum, ionospheric Hall currents, geomagnetic induction.

Abstract

Ground magnetometer data have been providing important knowledge of magnetic pulsations (or ULF waves) for more than a hundred years. With the advance of modern technologies, the accuracy of measurements is constantly improving. In addition, more arrays of magnetometer stations have been established. However, the usage of magnetometer arrays for studying magnetic pulsations has not been fully exploited. In this study, two recently developed methods for pulsation analysis are introduced. The first method involves an inversion technique that requires the observations from a chain of magnetometer stations located on a same latitude. This method can estimate several physical quantities related to the pulsation amplitude, namely the magnitude of the wave "event", the local time distribution, and the ground conductivity effect. The second method dubbed "the cross-phase technique" calculates the phase-difference spectrum of the signals measured at two closely separated stations on a same meridian. This technique has been found to be successful in "observing" the eigenfrequencies of magnetospheric field lines. It also provides an interesting opportunity to compare the field line resonance theory with the observations in detail.

1. Introduction

Ground magnetometer arrays have been providing important knowledge of magnetic pulsations (or ULF waves) in the magnetosphere. They are especially crucial for mid-latitude and low-latitude regions where spacecraft move too fast to provide useful measurements.

This article discusses two data analysis techniques developed recently. These techniques still have plenty of room for further improvements and they are potentially important in providing insights of the physics of pulsations. The first technique is an inverse method that can estimate the "intrinsic" wave amplitude at the latitude of consideration, the local time dependence of wave amplitude, and the ground conductivity effect through the same inversion procedure. The second technique is called the *cross-phase technique* that identifies the eigenfrequencies of field lines by the pattern of enhanced phase differences between the signals at two stations. It is a direct application of the field line resonance theory and it can be used as a "remote sensing" of the plasma density in the magnetosphere.

One of the common features for both techniques is that they require special consideration about the locations of the magnetometer stations. The inverse method analyzes the data from the stations on a same latitude. The cross-phase technique compares the phase difference in the wave signals that are measured at two closely spaced stations on a same longitude. The cross-phase technique also has a strict requirement for the synchronization of stations in order to determine phase differences accurately.

In the following, we first introduce the inverse method for equilatitude measurements, and then present the cross-phase technique for equilongitude measurements. A discussion on the possible future developments of the two methods will follow afterwards.

2. Inverse method for equilatitude measurements

This method uses the observations of wave power (or wave amplitude) from the ground stations located at the same latitude. The rationale is based on the high coherency in wave power modulation across the magnetometer arrays at mid and low latitudes [*Chi et al.,* 1994; *Chi et al.,* 1996]. At these latitudes, it is found that broad-band Pc 3-4 wave energy can often be observed in the daytime. Although the cause of the detailed modulation of wave power is not clear, there is evidence that the ultimate energy source is the upstream waves in the foreshock region [*Chi et al.,* 1994]. The waveform of signals on the other hand may not be coherent for all stations, and therefore the instantaneous wave amplitude is not used in calculation. The wave amplitude can be calculated by a Fourier transform of the signals in a time interval of 5–10 min (or an "event"), and thus accurate timing of magnetometer systems is not required here.

The technique is first discussed by *Chi et al.* [1996]. The original inversion model considers the wave amplitude observed on the ground, A, as a function of the magnitude of the wave event B, the local time dependence function $f(t)$, and the amplification of wave amplitude due to ground conductivity, σ. Their relationship can be written as

$$A = B\ f(t)\ \sigma. \tag{1}$$

If there are N_s stations located on a same latitude and N_e wave events for each station, the quantity

$$S = \sum_{i=1}^{N_e}\sum_{j=1}^{N_s}[A_{ij} - B_i f(t_{ij})\sigma_j]^2. \tag{2}$$

is expected to be minimal. In addition, if the local time dependence function $f(t)$ is expressed by a polynomial function

$$f(t) = 1 + \sum_{k=1}^{K} a_k t^k, \tag{3}$$

a set of nonlinear equations

$$\begin{aligned} \frac{\partial S}{\partial B_i} &= 0, \quad i = 1, 2, \ldots N_e. \\ \frac{\partial S}{\partial \sigma_j} &= 0, \quad j = 1, 2, \ldots N_s - 1. \\ \frac{\partial S}{\partial a_k} &= 0, \quad k = 1, 2, \ldots K. \end{aligned} \tag{4}$$

can be obtained by minimizing S. Note that there are only $N_s - 1$ independent variables for σ and one can define $\sigma_{N_s} \equiv 1$. The unknown parameters can be estimated by numerically solving the set of nonlinear equations (4). However, in the above equations, there are $N_e + N_s + K - 1$ unknowns, and the numerical calculation is not feasible if the number of events, N_e, becomes a large number. In fact, B can be replaced by the estimation

$$B_i^* = \frac{\sum_{j=1}^{N_s} \sigma_j f(t_{ij}) A_{ij}}{\sum_{j=1}^{N_s} [\sigma_j f(t_{ij})]^2} \tag{5}$$

since $\partial S/\partial B_i = 0$, and the number of parameters in optimization is a fixed number, $N_s + K - 1$, regardless how many events there are.

In this study, we present a different approach to estimate the unknown parameters without the computational power that is usually needed in solving the optimization problem. As in the previous study by *Chi et al.* [1996], the magnetic field data from the five northern stations in the Air Force Geophysical Laboratory (AFGL) array are used. All of the five stations are roughly aligned with the line of 55° corrected geomagnetic latitude, and their exact locations are listed in Table 1. The local time space of the stations is about 4 hours. From August to November 1978, 440 Ultra-Low-Frequency (ULF) wave events are selected, and they are further divided into three subgroups for the three different frequency bands: 7–15 mHz, 15–30 mHz, and 30–50 mHz.

Table 1. Locations of the five northern AFGL stations in corrected geomagnetic coordinates

Station	Latitude	Longitude
Newport (NEW)	55.2°	299.6°
Rapid City (RPC)	54.1°	317.3°
Camp Douglas (CDS)	56.3°	334.2°
Mt. Clemens (MCL)	55.8°	344.8°
Sudbury (SUB)	55.8°	1.9°

Different from the original analysis by *Chi et al.* [1996], a new data set is established by selecting the median wave amplitude as a function of local time and station. For a certain local time t, the median of the wave amplitude values within a two-hour bin centered at t is taken. Figure 1 shows the median wave amplitude for the 15–30 mHz frequency band at different local times. It can be seen that some stations (e.g., MCL) always observed stronger waves.

Since only the median values are taken for analysis, we can assume that the corresponding magnitudes of wave events are independent of local time. Therefore, the estimation of B is not needed. If we arbitrarily assume that $B = 1$, we know from (1) that $\sigma_j = A(t_{ij})/f(t_{ij})$. In Figure 1, all the five stations have data for local times $-4, -3, \cdots 3$, and we can have different estimates of σ_j for different local times. The mean value of σ_j is plotted in Figure 2, which shows a result consistent with the study by *Chi et al.* [1996].

Knowing the σ for each station, we can calibrate the wave amplitude by dividing it by σ. The calibrated value A/σ represents the wave amplitude expected to be observed on the ground when there is no difference in ground conductivity among the stations. For a local time t, the median value of the "calibrated" wave amplitude within a 2-hour bin centered at t can represent the local time dependence function $f(t)$. Figure 3 shows the $f(t)$ for the magnetic pulsations in three different frequency bands. For the lowest frequency band 7–15 mHz, the peak of $f(t)$ is located in the afternoon for the H component but in the morning for the D component. This distinction has been reported by *Bloom and Singer* [1995] using two years of AFGL data, but we are able to obtain the same result with much smaller amount of data by using the inverse method that can calibrate the ground conductivity effect.

Both B and $f(t)$ have important implications in space physics. Magnetic pulsations may be driven by the waves from the solar wind or excited internally in the magnetosphere. The magnitude of wave events B can be compared with other physical phenomena to reveal the important mechanisms that generate pulsations. It is analogous to compare the Kp index with solar wind parameters to understand the causes of geomagnetic disturbances. The difference is that Kp is an uncalibrated quantity comparing to B. The local time dependence function $f(t)$ is important in understanding the geometry of source energy and the ionospheric effect on pulsation amplitude.

3. Cross-phase technique for equilongitude measurements

The cross-phase spectrum provides a powerful tool to identify the eigenfrequencies of the magnetospheric field lines. It is found that the resonant frequencies cannot be easily identified by a simple station since the wave power spectrum usually consists of both the driving wave energy and the resonance energy. At the eigenfrequency of a field line centered between two neighboring stations in a north-south chain the phase difference maximizes [*Best et al.,* 1986; *Waters et al.,* 1991; *Green et al.,* 1993]. *Waters et al.* [1994] showed that the patterns of the maximum phase differences in the cross-phase spectrograms were observed consistently from day to day in the dayside region over baselines of about 100 km in the magnetic meridian.

To demonstrate the cross-phase technique, we first present the observations at two British stations, Durness (DU) and Loch Laggan (LL), located along the 60° geomagnetic meridian. The same event has been reported by *Chi and Russell* [1998]. On this meridian, the local time is roughly the same as the Universal Time (UT). The geomagnetic latitudes of DU and LL are 61.46° and 59.89°, respectively, and therefore the north-south separation between the two stations is 91 km. On May 9, 1979, broadband Pc 3-4 waves were observed at both stations. Figure 4a shows the wave power spectrogram of the magnetic field measureed at LL. Enhanced wave power was observed during the daytime over the entire Pc 3-4 band.

The cross-phase spectrum is the phase difference between the two time series in consideration as a function of frequency. Figures 4b-4d are the cross-phase spectrograms for the H, D, and Z components of the DU-LL pair on the same day. To better present the meaningful results, we set the phase difference to be 0 when the coherency between the two time series is less than 0.3. In addition, since the phase difference $\phi_{LL} - \phi_{DU}$ is mainly larger than 0, only positive values are shown. For the H component (Figure 4b), patterns of enhanced phase differences are seen at approximately 10, 22, 38, and 66 mHz in the daytime. These patterns are associated with the field line resonances in the magnetosphere, and the corresponding frequencies are the resonant frequencies for the field lines between the latitudes of the two stations [*Chi and Russell,* 1998]. Notice that the above frequencies cannot be identified as resonant frequencies from the power spectrogram (Figure 4a). The same patterns with even greater phase differences are seen in the Z component. In contrast the phase difference in the D component is much smaller and there exists no discernible pattern.

Waters et al. [1991] interpreted the cross-phase spectrum by using a two-oscillators model. Consider that the two field lines that have slightly different L-values are connected to two ground stations 1 and 2, where 1 denotes the station at a higher latitude. If we assume that the signals seen on the ground station is only caused by the oscillations of the field lines that connect to it, we can know the amplitude and phase responses for each field line when there is a common driving source. It can be shown that the phase difference $\phi_2 - \phi_1$ is the greatest at $\omega = (\omega_1 + \omega_2)/2$, where ω_1 and ω_2 are the eigenfrequencies of the two field lines (Figure 1 of *Waters et al.* [1991]).

Chi and Russell [1998] explained that Waters' two-oscillators model was physically incorrect and the cross-phase spectrograms should be interpreted by the field line resonance theory [*Chen and Hasegawa,* 1974] with additional consideration of the ionospheric effect. In this study, we use the conventional box model as proposed by *Southwood* [1974] for simplicity. All the field lines here are assumed to be straight and have the same length. The field direction is taken as the z axis. The medium is assumed to be inhomogeneous in the x direction, which is considered to represent the radially outward direction in the actual magnetosphere. The y direction can be determined by $\mathbf{y} = \mathbf{z} \times \mathbf{x}$. A surface wave with an wavenumber λ on the magnetosphere boundary can propagate evanescently inward and result in a field line resonance at an appropriate location. For the electric field in the y direction, the resonance can be expressed by the following equation [*Southwood,* 1974]:

$$\frac{d^2 E_y}{dx^2} + \frac{1}{x - x_0 - i\epsilon} \frac{dE_y}{dx} - \lambda^2 E_y = 0 \qquad (6)$$

where ϵ represents a small quantity due to the dissipation in the process. The solution of the above differential equation is

$$E_y(x) = C I_0(\lambda(x - x_0 + i\epsilon)) + D K_0(\lambda(x - x_0 + i\epsilon)) \qquad (7)$$

where I_0 and K_0 are modified Bessel functions. The electric field in the x direction is given by

$$E_x = -E_y \rho = -\frac{i\lambda}{(\omega/v_A)^2 - k^2 - \lambda^2} \frac{dE_y}{dx}. \qquad (8)$$

Figure 5 depicts the amplitudes and phases of E_x and E_y solved from (8) and (7) when appropriate boundary conditions are given. The resonant location x_0 is taken to be 0. It is clear that both E_x and E_y have maxima at the resonant point and their values are finite. The magnitude of E_x is much greater than that of E_y, and this indicates that the electric oscillations are mainly in the radial direction. The phases of both E_x and E_y have sudden changes at the resonant point. For the phase of E_x, the change is roughly π.

From the knowledge of E_x and E_y, the ionospheric currents can be easily estimated. If Σ_P and Σ_H stand for height-integrated Pedersen and Hall conductivity, we can write the Pedersen and Hall currents as

$$\begin{pmatrix} J_x \\ J_y \end{pmatrix} = \begin{pmatrix} \Sigma_P & \Sigma_H \\ -\Sigma_H & \Sigma_P \end{pmatrix} \begin{pmatrix} E_x \\ E_y \end{pmatrix}. \qquad (9)$$

Since the effect of the Pedersen currents cancels the incident wave, the magnetic oscillations on the ground only come from the contribution from the Hall currents. Figure 6 shows the four phases of Hall currents in one wave period. Since E_x dominates the electric field, the Hall-current oscillations are mainly in the y direction.

By using the Biot-Savart law, the ground signals of the magnetic field induced by the ionospheric Hall currents can be calculated, and the result is presented in Figure 7. Two cases for different ionospheric heights (h) are shown. The two plots on the left show the wave amplitude and the phase when $h = \epsilon$, where ϵ is representative of the resonance width. The wave amplitudes in the x and z components are comparable, and in the y component the wave amplitude is negligible because the ionospheric Hall currents are mainly in the same direction. The phase change across the resonance is the greatest in the Z component, and it is rather negligible in the D component. The two plots on the right show the same calculations but for the case when $h = 10\epsilon$. In this situation the ionospheric height is much greater and therefore the wave amplitudes are smaller than those in the previous case. In addition, the wave amplitude in the Z component is clearly smaller than that in the H component because the angle between the Earth's surface and the induced magnetic field is relatively smaller. The phase change is also smaller than in the previous case since the integrated effect that smears the difference in phase is stronger for the higher ionosphere.

The above calculation is simplistic because it does not consider the ground as a conductor. When ground conductivity is considered, the magnetic field on the ground can be viewed as the induction of the ionospheric current and its "image current" in the Earth. If an ionospheric current I is located at $z = h$ and a simple magnetostatic case is assumed, the image current I' is flowing in the opposite direction underground at $z = -h$ and its magnitude is $I(\mu_r - 1)/(\mu_r + 1)$ where μ_r is the relative permeability of the earth. For a good conductor, μ_r is usually large enough such that $I' \simeq -I$ and it can be immediately understood that B_z vanishes on the ground. In general, B_z is a non-zero quantity and it can be expressed as

$$B_z = \frac{\mu_0 I}{\pi(\mu_r + 1)} \frac{d}{d^2 + h^2} \qquad (10)$$

where d is the lateral distance from the current.

It should be noted that the above discussion of the net induction only serves a purpose as an approximation to reveal relevant physics. To estimate these geomagnetically induced currents more precisely, a much more sophisticated model that considers the complex skin depth and the finite length of ionospheric currents has been developed (e.g., *Pirjola and Viljanen* [1998]).

4. Discussion

We have presented two techniques that were developed in recent years for studying magnetic pulsations. The immediate use of the cross-phase technique is to estimate the plasma density in the magnetosphere as a part of understanding space weather, and the inverse method can be used as a tool to calibrate the wave amplitude observed on the ground. However, besides these practical purposes, the two methods are potentially important in advancing our understanding of the physics of magnetic pulsations and the field line resonance mechanism in the magnetosphere. Both techniques also require more research on their connection with theories.

For the inverse method, both the physical model and the optimization method demand further modifications. An apparent need is to consider σ as a tensor. Since the ground conductivity structure can be inhomogeneous, it is possible that the current flowing in the x direction in the ionosphere will induce magnetic field in both y and x directions on the ground. However, the inclusion of the off-diagonal terms in the σ tensor may greatly increase the number of parameters in the model and make the optimization much more difficult.

The optimal number of parameters is also an important issue in dealing with the optimization problem. In the original model [*Chi et al.,* 1996], the local time dependence function $f(t)$ is modeled by a fourth-order polynomial. A different order of polynomial or different functional forms are also possible choices, but a model selection criterion such as the Akaike Information Criterion [*Akaike,* 1974] should be used to determine the best model. The same consideration can also be applied to the inclusion of the σ tensor: for some stations the ground conductivity may be homogeneous and therefore the associated σ can be vectors rather than tensors in the model.

Another possible advancement is to include the magnetotelluric (MT) method used in geophysical exploration to obtain the detailed knowledge of ground conductivity. This will remove the σ parameters from the model and greatly reduce the difficulty in optimization. However, the MT method requires a high-density array of magnetometers in a rather small region, whereas the magnetometer arrays for studying space physics phenomena need to be more dispersive and cover a much wider area. It will be helpful for the scientists in these two fields to collaborate and coordinate the experiments that benefit both fields.

The comparison between the two-oscillators model proposed by *Waters et al.* [1991] and the conventional field line resonance model immediately raises the question of the number of resonant L-shells that exist in the magnetosphere. The two-oscillators model implies an infinite number of resonant L-shells, which is physically unrealistic. The field line resonance model has a resonance width that is associated with the dissapation of wave energy in the ionosphere, and therefore the number of resonances is expected to be finite. *Walker et al.* [1979] showed convincing cases by using radar observations that the Pc 5 in the outer magnetosphere had a resonance width of approximately 1° in latitude. However, the field line resonance theory does not tell us how many resonant L-shells there will be when the energy input is broad-band.

The cavity mode coupling with field line resonances [*Kivelson and Southwood,* 1985] also provides an alternative interpretation. In this scenario, field lines resonate only when the field line resonance frequency coincides with the cavity mode frequency, and thus the number of resonances is limited. However, different from the field line resonance model with finite resonance widths, the cavity resonance model predicts that not all harmonics of field line resonances may be seen at a certain latitude if the separation of two consecutive cavity modes is wide enough. Therefore, it is possible to distinguish the two different schemes by having the cross-phase spectrum from a chain of magnetometers on a same latitude.

So far the cross-phase technique has only considered the magnetometer stations located along the north-south direction. To apply the technique in the east-west direction and examine the azimuthal structure of field line resonances may also generate intriguing results. Except for the structure of small azimuthal wavelengths that cannot be seen on the ground due to the screening effect by the ionosphere [*Hughes and Southwood,* 1976], the phase differences may also tell us the azimuthal wave number. In an ideal condition as described in the field line resonance theory, the signals at two stations separated in the east-west direction are always coherent regardless the distance between them. However, this may not be true in reality and the information of coherence may hint to us what are the energy sources that generate resonances. Therefore, expanding the cross-phase analysis from one dimension to two dimensions is a natural trend as dense 2-D magnetometer arrays develop.

Acknowledgments. P. J. Chi is indebted to T. Higuchi of the Institute of Statistical Mathematics in Japan for developing the optimization algorithm of the inversion method.

References

Akaike, H., A new look at the statistical model identification, *IEEE Trans. Automatic Control, AC-19,* 716-723, 1974.

Best, A., S. M. Krylov, Yu. P. Kurchashov, Ya. S. Nikomarov, and V. A. Pilipenko, Gradient-time analysis of Pc3 pulsations, *Geomagn. and Aeronomy, 26,* 829, 1986.

Bloom, R. M., and H. J. Singer, Diurnal trends in geomagnetic noise power in the Pc 2 through Pc 5 bands at low geomagnetic latitudes, *J. Geophys. Res., 100,* 14943-14953, 1995.

Chen, L., and A. Hasegawa, A theory of long-period magnetic pulsations, 1. Steady state excitation of field line resonance, *J. Geophys. Res., 79,* 1024, 1974.

Chi, P. J., and C. T. Russell, An interpretation of the cross-phase spectrum of geomagnetic pulsations by the field line resonance theory, *Geophys. Res. Lett., 25,* 4445-4448, 1998.

Chi, P. J., C. T. Russell, and G. Le, Pc 3 and Pc 4 activity during a long period of low interplanetary magnetic field cone angle as detected across the Institute of Geological Sciences array, *J. Geophys. Res., 99,* 11127, 1994.

Chi, P. J., C. T. Russell, G. Le, W. J. Hughes, and H. J. Singer, A synoptic study of Pc 3,4 waves using the Air Force Geophysics Laboratory magnetometer array, *J. Geophys. Res., 101,* 13215-13224, 1996.

Green, A. W., E. W. Worthington, L. N. Baransky, E. N. Fedorov, N. A. Kurneva, V. A. Pilipenko, D. N. Shvetzov, A. A. Bektemirov, and G. V. Philipov, Alfven field line resonances at low latitudes ($L = 1.5$), *J. Geophys. Res., 98,* 15693, 1993.

Hughes, W. J., and D. J. Southwood, The screening of micropulsation signals by the atmosphere and ionosphere, *J. Geophys. Res., 81,* 3234-3240, 1976.

Kivelson, M. G., and D. J. Southwood, Resonant ULF waves: a new interpretation, *Geophys. Res. Lett., 12,* 49-52, 1985.

Pirjola, R., and A. Viljanen, Complex image method for calculating electric and magnetic fields produced by an auroral electrojet of finite length, *Ann. Geophysicae, 16,* 1434-1444, 1998.

Southwood, D. J., Some features of field line resonances in the magnetosphere, *Planet. Space Sci., 22,* 483-491, 1974.

Walker, A. D. M., R. A. Greenwald, W. F. Stuart, and C. A. Green, Stare auroral radar observations of Pc 5 geomagnetic pulsations, *J. Geophys. Res., 84,* 3373-3388, 1979.

Waters, C. L., F. W. Menk, and B. J. Fraser, The resonance structure of low latitude Pc3 geomagnetic pulsations, *Geophys. Res. Lett., 18,* 2293, 1991.

Waters, C. L., F. W. Menk, and B. J. Fraser, Low latitude geomagnetic field line resonances: Experiment and modeling, *J. Geophys. Res., 99,* 17547, 1994.

P. J. Chi and C. T. Russell, Institute of Geophysics and Planetary Physics, University of California, Los Angeles, Box 951567, Los Angeles, CA 90095. (e-mail: pchi@igpp.ucla.edu; ctrussel@igpp.ucla.edu)

This preprint was prepared with AGU's LaTeX macros v4. File two formatted March 12, 1999.

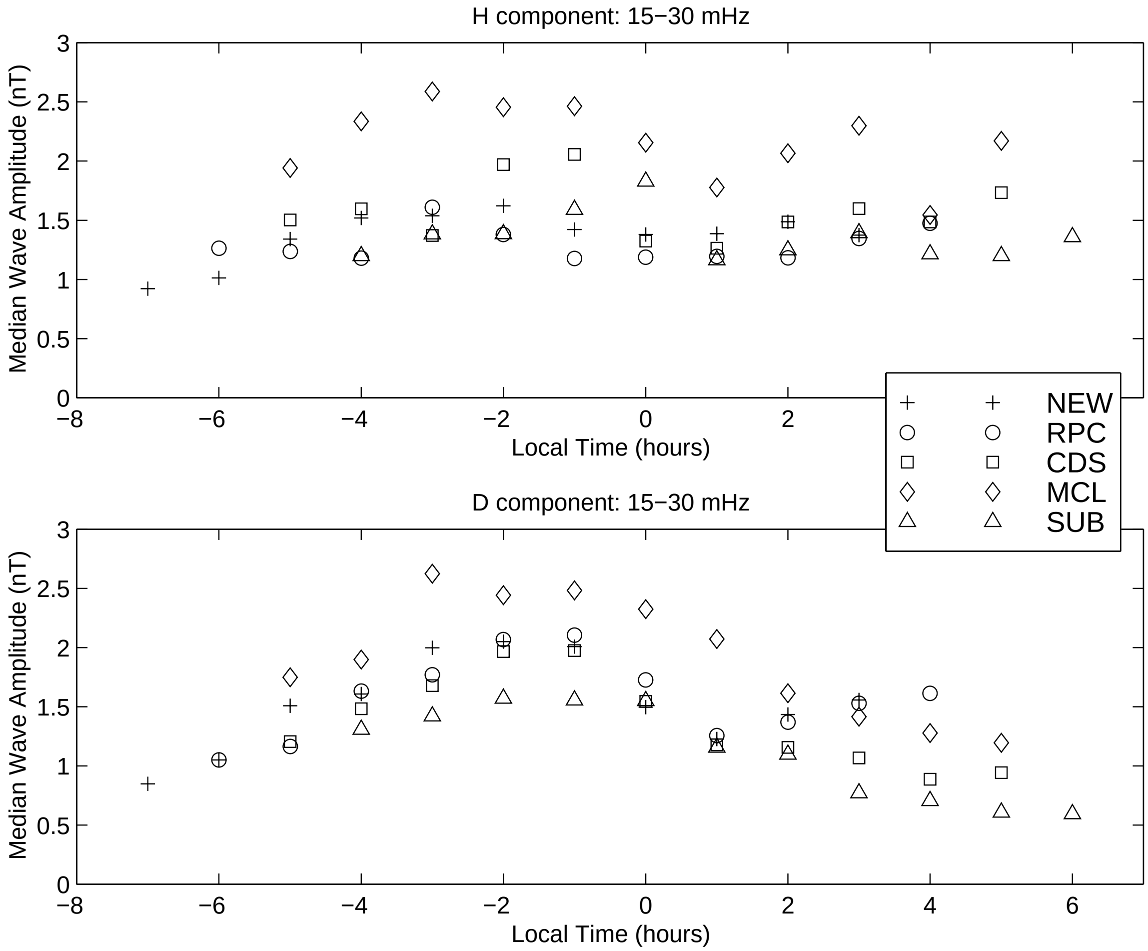

Figure 1. Median amplitude for the waves in the 15–30 mHz frequency band. There are 440 wave events selected for each station during August and November in 1978, and each data point represents the median wave amplitude within a 2-hour bin.

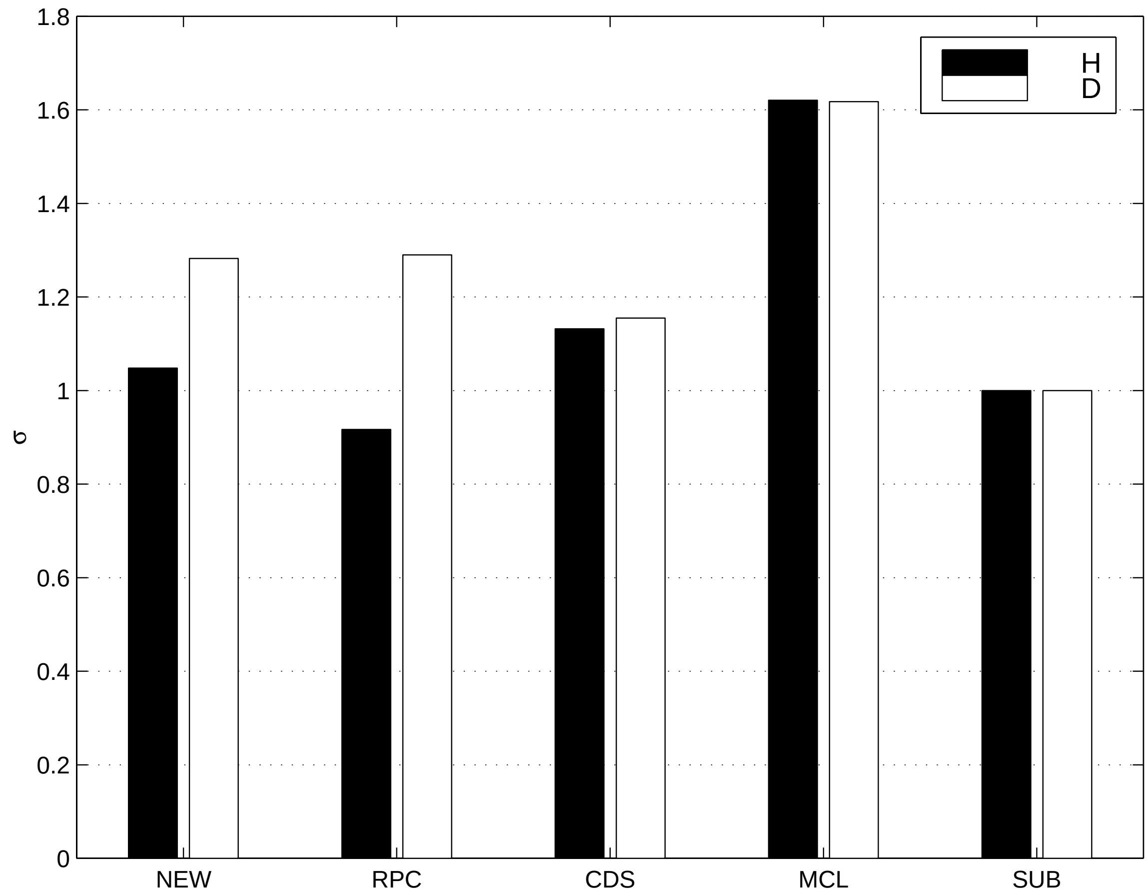

Figure 2. Amplification factors in the H and D components for the five northern AFGL stations. The σ for Sudbury (SUB) is set to be 1 for both components.

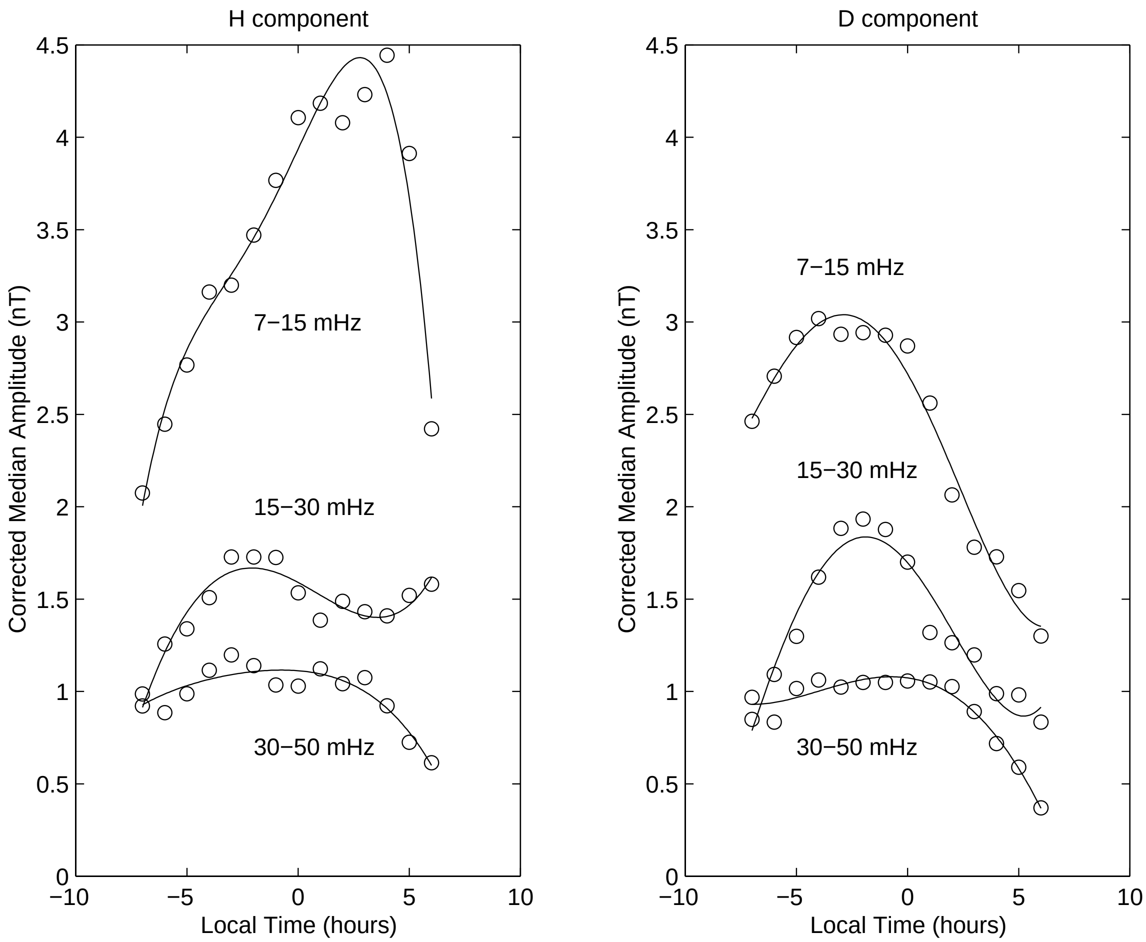

Figure 3. Corrected median wave amplitude representing the local time dependence function $f(t)$ for three different frequency bands. For each case, the solid line is the best fit by a fourth-order polynomial.

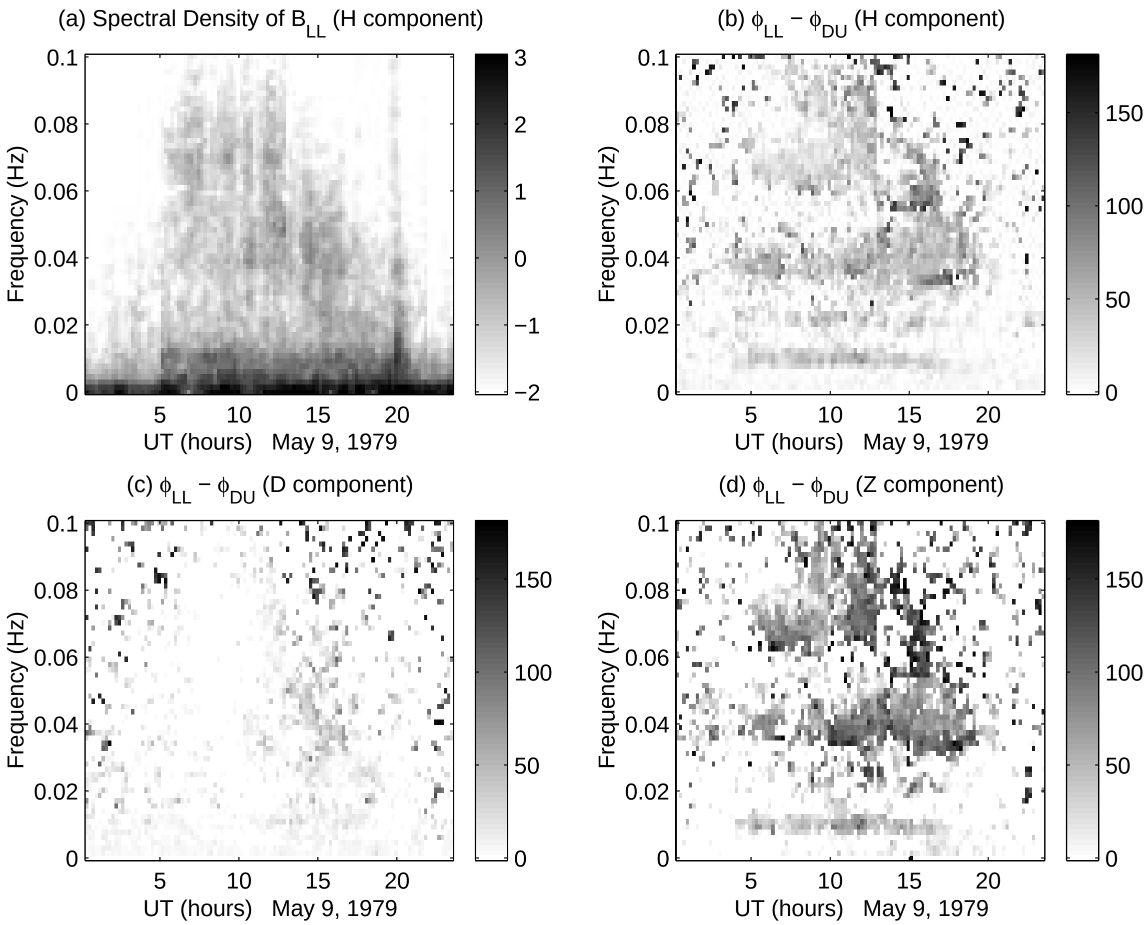

Figure 4. (a) Power spectrogram of B_H observed at LL. (b) Cross-phase spectrogram for the station pair DU-LL in the H component. (c) and (d) are the same as (b) except for the D component and Z component, respectively.

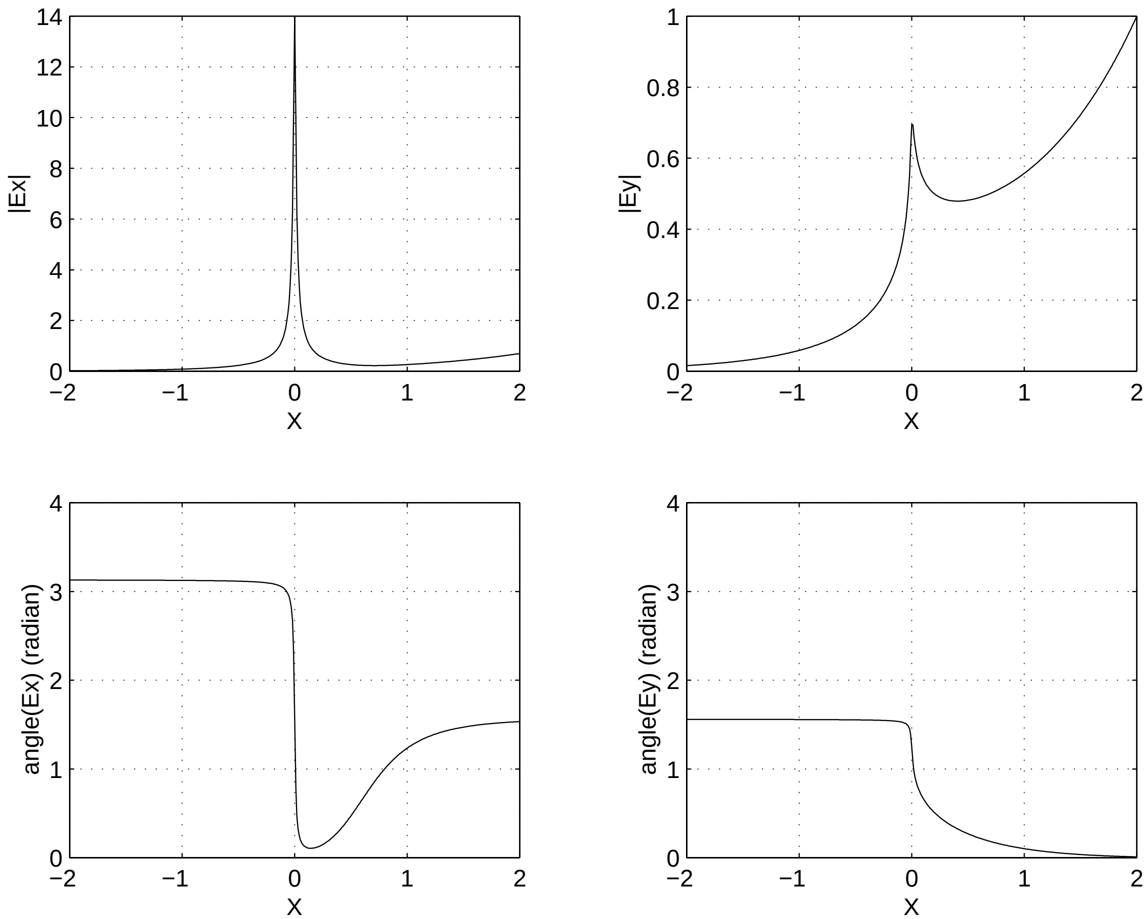

Figure 5. Amplitude and phase (angle) as functions of x for E_x and E_y calculated from (7) and (8).

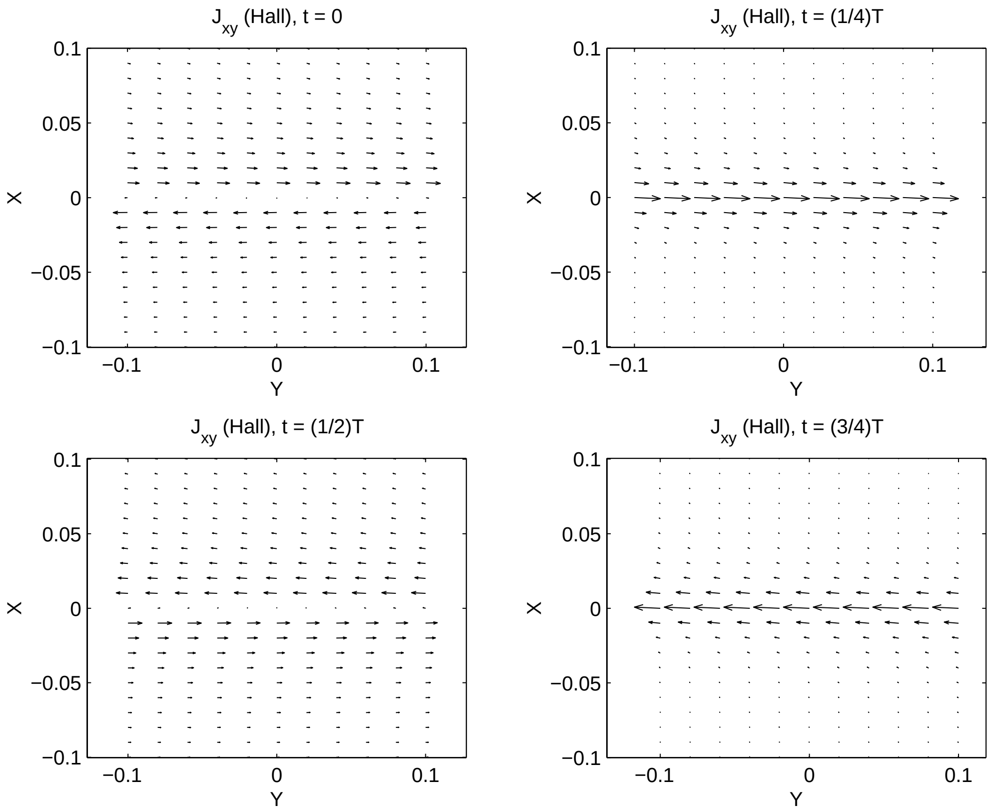

Figure 6. Ionospheric Hall currents excited by a field line resonance at four different phases in a wave cycle.

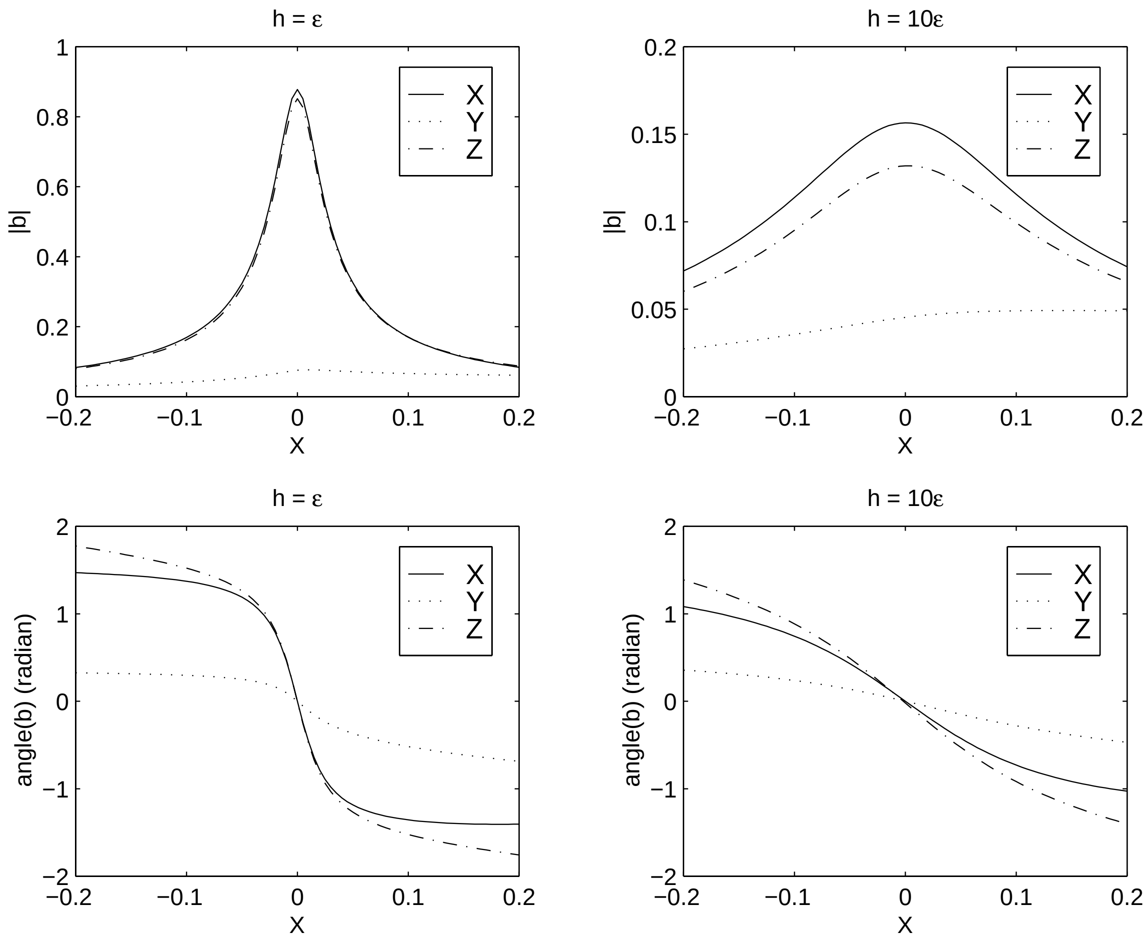

Figure 7. Wave amplitude and phase of the magnetic field oscillations on the ground induced by a field line resonance. (Left) When $h = \varepsilon$. (Right) When $h = 10\varepsilon$.